PHYSICAL REVIEW C **90**, 014320 (2014)

# Low-lying isomeric states in $^{80}$Ga from the $\beta^-$ decay of $^{80}$Zn

R. Lică,[1] N. Mărginean,[1] D. G. Ghiţă,[1] H. Mach,[2,3] L. M. Fraile,[2] G. S. Simpson,[4,5,6] A. Aprahamian,[7] C. Bernards,[8,9] J. A. Briz,[10] B. Bucher,[7] C. J. Chiara,[11,12] Z. Dlouhý,[13,*] I. Gheorghe,[1] P. Hoff,[14] J. Jolie,[8] U. Köster,[15] W. Kurcewicz,[16] R. Mărginean,[1] B. Olaizola,[2] V. Paziy,[2] J. M. Régis,[8] M. Rudigier,[8] T. Sava,[1] M. Stănoiu,[1] L. Stroe,[1] and W. B. Walters[11]

[1]*"Horia Hulubei" National Institute of Physics and Nuclear Engineering, Bucharest, Romania*
[2]*Grupo de Física Nuclear, Facultad de CC. Físicas, Universidad Complutense, CEI Moncloa, 28040 Madrid, Spain*
[3]*National Centre for Nuclear Research, BP1, ul. Hoża 69, 00-681 Warsaw, Poland*
[4]*LPSC, Université Joseph Fourier Grenoble 1, CNRS/IN2P3, Institut National Polytechnique de Grenoble, F-38026 Grenoble Cedex, France*
[5]*School of Engineering, University of the West of Scotland, Paisley, PA1 2BE, United Kingdom*
[6]*Scottish Universities Physics Alliance, University of Glasgow, Glasgow, G12 8QQ, United Kingdom*
[7]*Department of Physics, University of Notre Dame, Notre Dame, Indiana 46556, USA*
[8]*Institut für Kernphysik, Köln, Germany*
[9]*Wright Nuclear Structure Laboratory, Yale University, New Haven, Connecticut 06511, USA*
[10]*Instituto de Estructura de la Materia, CSIC, E-28006 Madrid, Spain*
[11]*Department of Chemistry and Biochemistry, University of Maryland, College Park, Maryland 20742, USA*
[12]*Physics Division, Argonne National Laboratory, Argonne, Illinois 60439, USA*
[13]*Nuclear Physics Institute, AS CR, Řež, Czech Republic*
[14]*Department of Chemistry, University of Oslo, Oslo, Norway*
[15]*Institut Laue-Langevin, Grenoble, France*
[16]*Institute of Experimental Physics, University of Warsaw, Warsaw, Poland*

(Received 27 May 2014; published 28 July 2014)

A new level scheme of $^{80}$Ga has been determined. This nucleus was populated following the $\beta^-$ decay of $^{80}$Zn at ISOLDE, CERN. The proposed level scheme is significantly different compared to the previously reported one and contains 26 levels up to 3.4 MeV in excitation energy. The present study establishes that the previously identified 1.9-s $\beta^-$-decaying $6^-$ isomer is the ground state of $^{80}$Ga and the 1.3-s $\beta^-$-decaying $3^-$ isomer lies at an excitation energy of 22.4 keV. A new isomeric level was identified at 707.8 keV and its half-life was measured to be 18.3(5) ns, allowing the 685.4-keV transition de-exciting this state to be assigned an $M2$ multipolarity. The newly measured spectroscopic observables are compared with shell-model calculations using the jj44bpn and JUN45 interactions.

DOI: 10.1103/PhysRevC.90.014320 PACS number(s): 21.10.Tg, 23.20.Lv, 23.40.−s, 27.50.+e

## I. INTRODUCTION

The recent availability of clean, intense beams of radioactive isotopes close to the presumed doubly magic nucleus $^{78}$Ni has triggered renewed interest in this region. As it is the region around the most neutron rich doubly magic nucleus (highest $N/Z$ ratio) currently accessible for experimental studies, comparisons between spectroscopic data on the nuclei here and state-of-the-art shell-model calculations play a key role in assessing the impact of neutron excess on effective nucleon-nucleon interactions. Spectroscopic information also allows the evolution of single-particle orbit energies to be followed as a function of $Z$ and $N$. In the present work $\gamma$ decays of the three-valence-proton, one-valence-hole nucleus $^{80}$Ga have been observed and compared to the predictions of shell-model calculations, allowing a sensitive test of neutron-proton interactions in this region.

Nuclear structure is an important input into rapid neutron-capture-process ($r$-process) nucleosynthesis calculations. The key parameters of interest are ground- and isomeric-state half-lives and delayed-neutron emission probabilities, which are all influenced by shell structure. The observed $r$-process abundance patterns traditionally consists of three main peaks around $A \sim 80$, 130, and 195, associated with the $N = 50$, 82, and 126 closed neutron shells. All indications are that the peak around $A = 80$ must have formed in very different astrophysical conditions than the higher mass peaks [1]. Any erosion of the $Z = 28$ and $N = 50$ shell closures would have an obvious impact on the direction and speed of the $r$-process around the $A \sim 80$ abundance peak. Possible experimental evidence for the less-than-robust nature of these shells includes mass measurements, which indicate that $^{78}$Ni is not the most tightly bound nucleus of this region [2].

A recent collinear laser-spectroscopy experiment [3] has identified a $3^-$ isomeric state in $^{80}$Ga, lying at an unknown energy above the proposed $6^-$ ground state. Half-lives for these two $\beta$-decaying states were recently reported in Ref. [4]. In the present work, the excitation energy of the $3^-$ isomeric state of $^{80}$Ga is determined from the observed $\gamma$-decay scheme and the positions of several levels are revised. The data from the present and previous works are in good agreement with shell-model calculations performed using the jj44bpn and JUN45 interactions.

[*]Deceased.

 

TABLE I. Gamma-ray transitions in $^{80}$Ga, as found in the present work, associated with the level scheme shown in Fig. 1. The transition intensities are normalized to that of the 712-keV $\gamma$ ray, taken as 100. For absolute intensity per 100 decays, multiply the relative intensity by 0.41(6). The tentative $\gamma$ rays are marked with $^t$. The strong transitions were calculated from the prompt $\gamma$ singles spectrum and the weaker ones from coincidence spectra. All the errors are based on statistical uncertainties and fitting approximations.

| $E_\gamma$ | $I_\gamma$ | Assignment | | | |
|---|---|---|---|---|---|
| (keV) | | $E_{\text{initial}}$ | $E_{\text{final}}$ | $J_i^\pi$ | $J_f^\pi$ |
| 74.8(1) | 10.8(2) | 97.1 | 22.4 | — | $3^-$ |
| 75.8(1)$^t$ | <0.2 | 1526.0 | 1450.0 | — | $1^+$ |
| 93.4(1) | 3.2(6) | 1450.0 | 1356.5 | $1^+$ | — |
| 151.7(1)$^t$ | <0.2 | 1141.9 | 990.0 | — | — |
| 154.7(1) | 0.3(1) | 1141.9 | 987.1 | — | — |
| 159.5(1) | 1.2(3) | 1450.0 | 1290.4 | $1^+$ | — |
| 169.6(1) | 1.4(3) | 1526.0 | 1356.5 | — | — |
| 174.0(1) | 5.6(6) | 577.3 | 403.4 | — | — |
| 176.6(1) | 10.1(10) | 911.3 | 734.7 | — | — |
| 190.5(1) | 2.3(2) | 1141.9 | 951.4 | — | — |
| 203.6(1) | 0.3(1) | 1193.8 | 990.0 | — | — |
| 225.7(1) | 1.2(2) | 1526.0 | 1300.5 | — | — |
| 243.5(1) | 0.9(2) | 951.4 | 707.8 | — | $(1^+)$ |
| 282.21(5) | 4.1(4) | 990.0 | 707.8 | — | $(1^+)$ |
| 282.7(1) | 0.6(2) | 1193.8 | 911.3 | — | — |
| 306.4(1) | 0.2(1) | 403.4 | 97.1 | — | — |
| 308.3(1) | 0.4(1) | 1450.0 | 1141.9 | $1^+$ | — |
| 312.13(5) | 12.4(2) | 1526.0 | 1213.9 | — | — |
| 332.17(5) | 2.6(4) | 1526.0 | 1193.8 | — | — |
| 373.2(1) | 0.2(1) | 1526.0 | 1152.7 | — | — |
| 403.47(3) | 4.3(5) | 403.4 | 0.0 | — | $6^-$ |
| 406.9(2) | 0.8(2) | 1141.9 | 734.7 | — | — |
| 433.9(1) | 2.2(4) | 1141.9 | 707.8 | — | $(1^+)$ |
| 444.9(1) | 0.8(1) | 1356.5 | 911.3 | — | — |
| 459.9(1)$^t$ | <0.2 | 1450.0 | 990.0 | $1^+$ | — |
| 462.72(2) | 11.1(1) | 1450.0 | 987.1 | $1^+$ | — |
| 468.3(1) | 2.2(6) | 2560.4 | 2092.1 | $(1^+)$ | $1^+$ |
| 480.1(1) | 0.7(1) | 577.3 | 97.1 | — | — |
| 518.3(1) | 1.0(2) | 2044.5 | 1526.0 | — | — |
| 538.87(5) | 1.3(2) | 1526.0 | 987.1 | — | — |
| 566.20(5) | 10(1) | 2092.1 | 1526.0 | $1^+$ | — |
| 575.3(1) | 0.4(1) | 1152.7 | 577.3 | — | — |
| 577.7(2) | 0.2(1) | 577.3 | 0.0 | — | $6^-$ |
| 594.9(1)$^t$ | 0.3(1) | 2044.5 | 1450.0 | — | $1^+$ |
| 614.66(5) | 13.3(4) | 1526.0 | 911.3 | — | — |
| 621.8(1) | 1.7(3) | 1356.5 | 734.7 | — | — |
| 632.5(1) | 3.5(4) | 2677.0 | 2044.5 | $1^+$ | — |
| 636.6(1) | 4.5(5) | 1213.9 | 577.3 | — | — |
| 642.3(1) | 30(3) | 2092.1 | 1450.0 | $1^+$ | $1^+$ |
| 685.4(1) | 36(4) | 707.8 | 22.4 | $(1^+)$ | $3^-$ |
| 688.0(1) | 1.8(3) | 2044.5 | 1356.5 | — | — |
| 712.3(1) | 100(10) | 734.7 | 22.4 | — | $3^-$ |
| 723.2(8)$^t$ | <0.2 | 1300.5 | 577.3 | — | — |
| 715.2(1) | 77(21) | 1450.0 | 734.7 | $1^+$ | — |
| 735.6(1) | 2.2(4) | 2092.1 | 1356.5 | $1^+$ | — |
| 742.0(1) | 21(2) | 1450.0 | 707.8 | $1^+$ | $(1^+)$ |
| 791.3(1) | 4.0(6) | 1526.0 | 734.7 | — | — |
| 802.0(1) | 0.8(2) | 2092.1 | 1290.4 | $1^+$ | — |
| 814.2(1) | 1.6(2) | 911.3 | 97.1 | — | — |
| 818.2(1) | 1.1(3) | 1526.0 | 707.8 | — | $(1^+)$ |
| 878.2(2) | 1.0(2) | 2092.1 | 1213.9 | $1^+$ | — |
| 888.9(1) | 5.7(6) | 911.3 | 22.4 | — | $3^-$ |
| 928.8(2) | 13.6(15) | 951.4 | 22.4 | — | $3^-$ |
| 950.5(2) | 1.3(3) | 2092.1 | 1141.9 | $1^+$ | — |
| 964.8(2) | 32(3) | 987.1 | 22.4 | — | $3^-$ |
| 1034.3(2) | 9.2(10) | 2560.4 | 1526.0 | $(1^+)$ | — |
| 1057.3(3) | 0.6(2) | 2044.5 | 987.1 | — | — |
| 1104.9(2) | 5.4(7) | 2092.1 | 987.1 | $1^+$ | — |
| 1110.3(2) | 1.8(6) | 2560.4 | 1450.0 | $(1^+)$ | $1^+$ |
| 1116.7(2) | 9.0(10) | 1213.9 | 97.1 | — | — |
| 1150.9(2) | 22(2) | 2677.0 | 1526.0 | $1^+$ | — |
| 1171.5(2) | 3.9(5) | 1193.8 | 22.4 | — | $3^-$ |
| 1203.3(2) | 1.1(2) | 1300.5 | 97.1 | — | — |
| 1226.9(2) | 3.2(8) | 2677.0 | 1450.0 | $1^+$ | $1^+$ |
| 1267.9(2) | 5.9(7) | 1290.4 | 22.4 | — | $3^-$ |
| 1296.2(2) | 1.7(6) | 2822.1 | 1526.0 | — | — |
| 1320.6(2) | 2.0(5) | 2677.0 | 1356.5 | $1^+$ | — |
| 1334.0(2) | 9.9(11) | 1356.5 | 22.4 | — | $3^-$ |
| 1357.2(2) | 2.1(4) | 2092.1 | 734.7 | $1^+$ | — |
| 1366.4(2) | 1.0(4) | 2560.4 | 1193.8 | $(1^+)$ | — |
| 1372.0(2) | 1.6(3) | 2822.1 | 1450.0 | — | $1^+$ |
| 1384.3(2) | 1.4(3) | 2092.1 | 707.8 | $1^+$ | $(1^+)$ |
| 1386.6(2) | 1.9(4) | 2677.0 | 1290.4 | $1^+$ | — |
| 1418.4(2) | 0.8(1) | 2560.4 | 1141.9 | $(1^+)$ | — |
| 1427.5(2) | 3.8(8) | 1450.0 | 22.4 | $1^+$ | $3^-$ |
| 1503.6(3) | 9.6(11) | 1526.0 | 22.4 | — | $3^-$ |
| 1570.2(3) | 1.6(2) | 2560.4 | 990.0 | $(1^+)$ | — |
| 1573.5(3) | 0.4(2) | 2560.4 | 987.1 | $(1^+)$ | — |
| 1608.8(3)$^t$ | <0.2 | 2560.4 | 951.4 | $(1^+)$ | — |
| 1726.5(3)$^t$ | <0.2 | 2677.0 | 951.4 | $1^+$ | — |
| 1825.5(3) | 0.7(2) | 2560.4 | 734.7 | $(1^+)$ | — |
| 1834.9(3) | 2.6(2) | 2822.1 | 987.1 | — | — |
| 1871.3(3)$^t$ | <0.2 | 2822.1 | 951.4 | — | — |
| 2021.8(3) | 1.3(3) | 2044.5 | 22.4 | — | $3^-$ |
| 2378.1(3) | 0.8(2) | 3329.4 | 951.4 | — | — |
| 2428.6(3) | 0.5(1) | 3380.0 | 951.4 | — | — |

## II. EXPERIMENT

Excited states in $^{80}$Ga were populated following the $\beta^-$ decay of $^{80}$Zn isotopes at ISOLDE, CERN. Two similar experiments have been performed using slightly different production methods for $^{80}$Zn. In the first experiment, in 2009, $^{80}$Zn nuclei were produced by 1.4-GeV protons impinging directly on a thick uranium carbide target. This production mechanism was responsible for the strong presence of proton-rich impurities at mass 80. In the second experiment, in 2011, the proton beam hit a neutron converter, which produced fast neutrons. These then induced fission in the uranium carbide target, producing mostly neutron-rich fragments. The reaction products diffused from the ∼2000°C hot target via a chemically selective quartz transfer line into a tungsten ionizer, where resonant laser ionization was used to produced an intense, pure Zn ion beam [5–7]. After extraction and acceleration to 40 keV, the ISOLDE

high-resolution separator was used to mass select an $A = 80$ beam. Around 20 000 ions/s were sent to an aluminium catcher foil at the center of an array of $\beta$ and $\gamma$ detectors.

The detection system consisted of a 3-mm-thick NE111 plastic scintillator positioned less than 0.5 mm behind the Al foil at the ion collection point. This detector was used as a fast-response $\beta$ detector. The thickness of the plastic scintillator was chosen to yield an almost uniform time response to $\beta$ particles within a wide range of energies. Two conical, 1.5-in-long $LaBr_3$(Ce) crystals were used as fast-response $\gamma$ detectors. In addition, two HPGe detectors were present, with relative efficiencies of about 60%, covering an energy range of 30 to 4000 keV. These were used to provide a unique selection of $\gamma$-decay branches in $\beta$-$\gamma(E)$-$\gamma(t)$ fast-timing measurements [8,9] and to study $\gamma$-$\gamma$ coincidences, in order to determine the level scheme. A 16-parameter PIXIE-4 digital data acquisition (DAQ) system was used to collect energy signals from all five detectors, along with the time of arrival of the proton pulse on the target or converter. Moreover, the DAQ system also collected five time-to-amplitude converter (TAC) signals. Four of the TACs were started by the $\beta$ signal and stopped by each of the $\gamma$ detectors, whereas the fifth TAC was started by one $LaBr_3$(Ce) detector and stopped by the other. The TAC range for the fast-timing detectors was set to 50 ns, whereas the ones stopped by Ge detectors had a range of 2 $\mu$s. The energy and efficiency calibrations of the $\gamma$ detectors were determined by using sources of $^{133,140}$Ba, $^{137}$Cs, and $^{152}$Eu. For the present analysis, only the $\beta$ and HPGe detector signals from the 2011 experiment and $\beta$-$LaBr_3$(Ce) coincidences from the 2009 experiment are used.

## III. EXPERIMENTAL RESULTS

New $\gamma$ transitions in $^{80}$Ga were assigned from coincidences with previously reported ones in Refs. [10,11]. A total of 86 transitions in this nucleus are reported in Table I. The level scheme of $^{80}$Ga, as determined in the present work, shown in Fig. 1, is in good agreement with the previously published ones in Refs. [10,11], with one exception. The placement of the 403-keV $\gamma$ ray in the level scheme shown in Fig. 3 of [10] is questioned. No coincidences with the 282- and 614-keV transitions are observed in the gated spectra of the present work, shown in Fig. 2. Therefore the 75-, 174-, 312-, 403-, 637-, and 1117-keV $\gamma$ rays are repositioned in our new level scheme so that the 403-keV transition directly feeds the ground state. The ground state now lies 22.4 keV below the next excited level. The new ground state is determined based on the fact that the aforementioned $\gamma$ rays are coincident with 1151-, 1034-, and 566-keV transitions and that the 403-, 174-, 637-, and 312-keV $\gamma$ rays are mutually coincident, hence comprise a cascade. One possible arrangement is that the four transitions succeed each other starting from the 1526-keV level. This

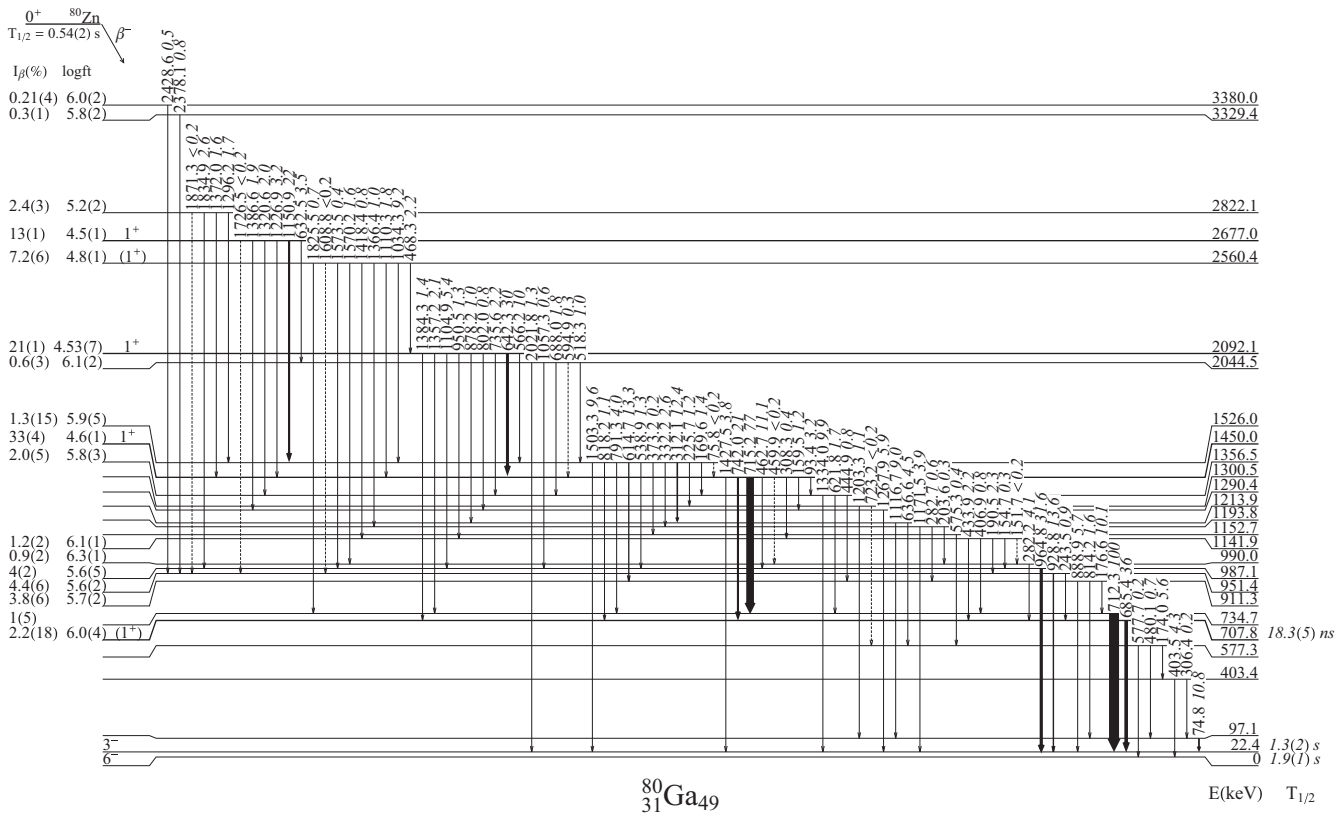


FIG. 1. Level scheme of $^{80}$Ga populated in the $\beta$ decay of $^{80}$Zn. There are a total of 86 $\gamma$ transitions. The dotted lines indicate weak transitions. The transition labels show the energy value and the relative $\gamma$ intensity. For absolute intensity per 100 decays, multiply by 0.41(6). $I_\beta$ values were determined by an intensity balance between the $\gamma$ rays feeding and de-exciting each level. The log $ft$ values were calculated using $Q_\beta = 7290$ keV from [21]. Half-lives for the $6^-$ and $3^-$ states are taken from [4].

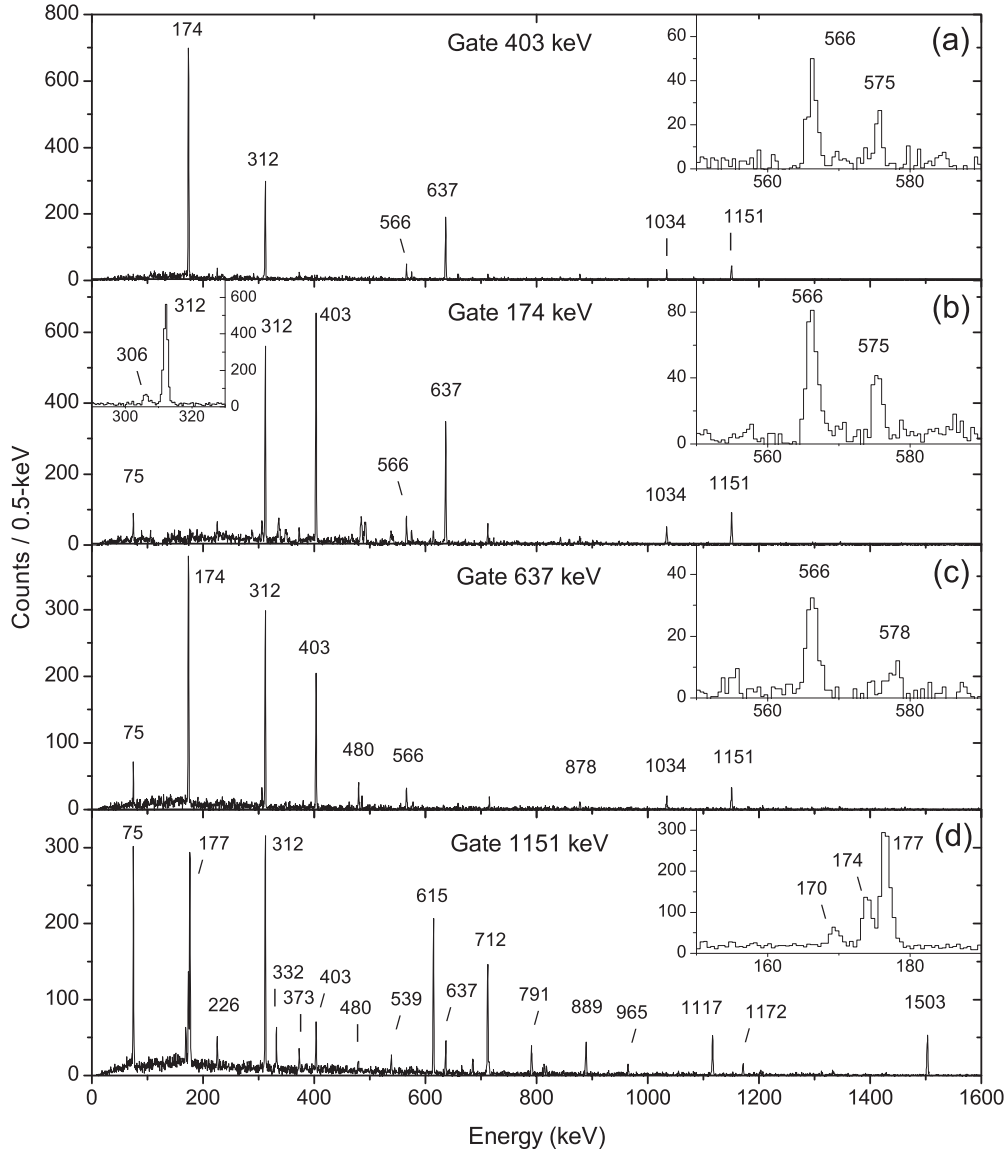


FIG. 2. HPGe $\gamma$-$\gamma$ coincidence spectra containing transitions from $^{80}$Ga with gates on the relevant 403-, 174-, 637-, and 1151-keV transitions.

ordering was confirmed by coincidences with additional newly discovered transitions. The present level scheme, combined with the results reported in [3], suggest a 1.9-s $6^-$ ground state, which $\beta$ decays to feed the $8^+_1$ level of $^{80}$Ge, as reported in [12]. The first excited state should then have spin and parity $3^-$, corresponding to the long-lived isomer reported in [3].

The conversion coefficient for the 74.8-keV transition between the 97.1- and 22.4-keV levels is determined to be $\geqslant$0.15(18), from the intensity balance in the level scheme and with the assumption that the 97.1-keV level is not directly $\beta$ fed. On the other hand, the conversion coefficient was found to be equal to 0.20(20) from the coincidence probabilities involving the 74.8-keV transition. We therefore adopt a conversion coefficient of $\leqslant$0.40 for the 74.8-keV $\gamma$ ray. The multipolarity of this transition can be assigned as $E1$ or $M1$, from a comparison with theoretical conversion coefficients [$\alpha(E1) = 0.15$, $\alpha(M1) = 0.15$, $\alpha(E2) = 2.08$, and $\alpha(M2) = 2.10$] [13]. Consequently, $4^-$ is the most likely spin and parity assignment for this level.

An analysis of the time-difference spectra between the $LaBr_3$(Ce) detectors and the fast plastic scintillator showed a long-lived decay component which corresponds to the 685.4-keV transition, connecting the 707.8-keV level and 22.4-keV $3^-$ level. As shown in Fig. 3, a gate on the 742.0-keV transition in the HPGe spectra was used to isolate the 685.4-keV transition in the $LaBr_3$(Ce) detectors. The half-life observed, $T_{1/2} = 20.9(35)$ ns, is significantly longer than that of the prompt 642.3-keV line. It was therefore possible to completely isolate the 685.4-keV transition, by selecting only delayed $LaBr_3$(Ce) events, with respect to prompt $\beta$-$LaBr_3$(Ce) ones. Having no gating condition on the HPGe detectors provided better statistics and hence a more precise half-life measurement, yielding $T_{1/2} = 18.3(5)$ ns, which is the adopted value. In Table II, a comparison is shown between

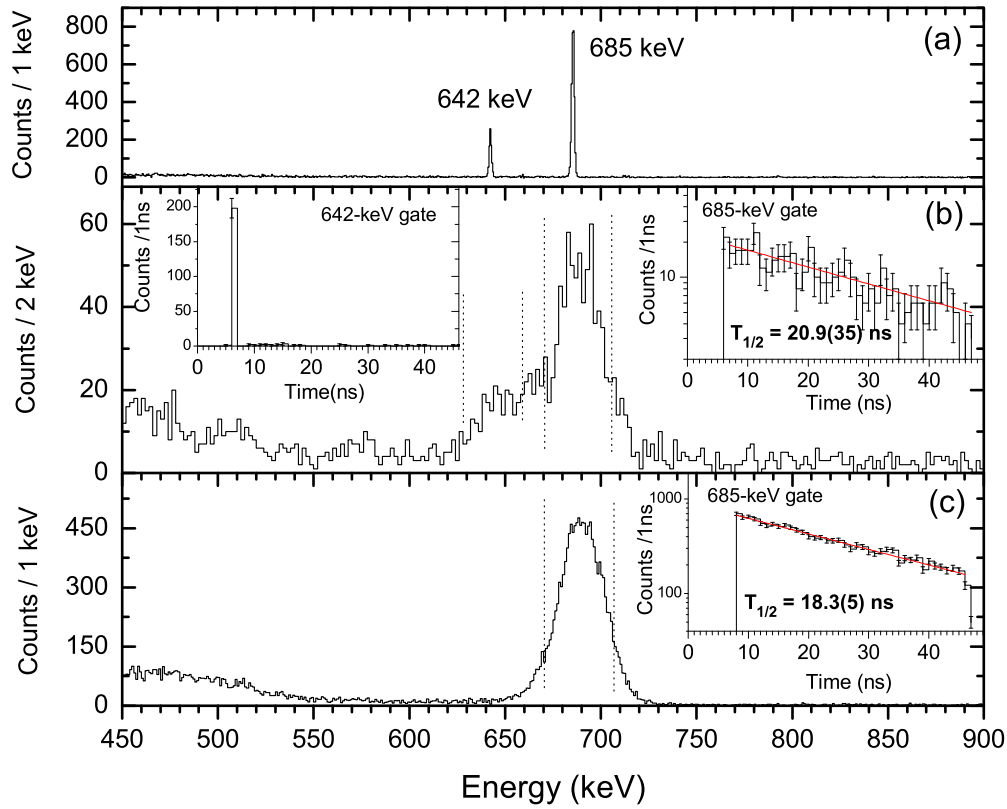


FIG. 3. (Color online) (a) 742.0-keV gate from $\gamma$-$\gamma$ HPGe coincidence spectra. (b) 742.0-keV gate on HPGe in the $\beta$-$\gamma_{\mathrm{HPGe}}$-$\gamma_{\mathrm{LaBr_3}}$(Ce) spectra. The time was recorded with time-to-amplitude converters between the plastic scintillator ($\beta$ detector) and each $LaBr_3$(Ce) detector. The time spectra have an offset of 6 ns. (c) Delayed ($T > 8$ ns) $\beta$-gated spectra in $LaBr_3$(Ce).

the reduced transition probabilities for different possible multipolarities and the recommended upper limits [14]. Only an $M2$ multipolarity has a reduced transition probability of the same order of magnitude as the recommended upper limits. The very low reduced transition probabilities for an $E1$, $M1$, or $E2$ transition would suggest extremely hindered transitions, which are highly unlikely in this mass region. The $E3$ or $M3$ reduced transition probabilities are more than one or four orders of magnitude higher, respectively. Based on these observations, we propose a ($1^+$) assignment for the 707.8-keV level, even in the absence of observed strong $\beta$ feeding to confirm this. This assumption is in agreement with the previous tentative assignment [10].

The $1^+$ spin and parity assignments for the levels at 2677.0, 2092.1, and 1450.0 keV are based on $\log ft$ values (indicated in Fig. 1) extracted for these strongly $\beta$-fed levels. The $1^+$ assignment for the 2560.4-keV level is only tentative.

TABLE II. Comparison between reduced transition probabilities $B(X\lambda)$ for the measured 685.4-keV transition, with an 18.3(5)-ns half-life, for an $A = 80$ nucleus, and recommended upper limits (RUL) taken from [14].

| $X\lambda$ multipolarity | $B(X\lambda)$ (W.u.) | |
|---|---|---|
| | Measured | RUL [14] |
| $E1$ | $6.2(2)\times10^{-8}$ | 0.01 |
| $M1$ | $3.7(1)\times10^{-6}$ | 3 |
| $E2$ | $9.9(3)\times10^{-3}$ | 300 |
| $M2$ | 0.60(2) | 1 |
| $E3$ | $2.44(7)\times10^{3}$ | 100 |
| $M3$ | $1.48(4)\times10^{5}$ | 10 |

## IV. COMPARISON WITH SHELL-MODEL CALCULATIONS

In Ref. [15], the authors address the quenching of the $Z = 28$ gap around $^{78}$Ni in the shell-model framework with a large valence space containing $pf$ orbitals for protons and $pf_{5/2}g_{9/2}$ orbitals for neutrons, including the single-particle orbits $p_{3/2}$, $f_{5/2}$, $p_{1/2}$, and $g_{9/2}$. The calculations are able to correctly reproduce the systematics of low-lying states and magnetic moments in Cu isotopes, underlining the importance of including protons from the $f_{7/2}$ shell. It is also claimed that the $Z = 28$ shell closure is diminished when the neutron $g_{9/2}$ orbital is filled, thus pointing to the relevance of proton core excitations in order to understand the structure of neutron-rich nuclei in the vicinity of $^{78}$Ni.

Honma and co-workers [16] have developed the JUN45 effective interaction for nuclei in the upper part of the $pf$ shell. The model space for both protons and neutrons contains the $pf_{5/2}g_{9/2}$ orbitals and the effective core is $^{56}$Ni. A more recent effective interaction (jj44bpn), using the same valence space and core as the JUN45 interaction, was developed by Brown

and Lisetskiy [17]. Calculations for $^{71-78}$Ga were published in [18] with the remark that, for the heavier isotopes, the jj44bpn interaction is quantitatively better than JUN45.

We have performed shell-model calculations with the NUSHELLX@MSU code [19] using the jj44bpn and JUN45 effective interactions. In Fig. 4, a comparison is shown between the shell-model calculations and the present experimental results for $^{80}$Ga. The calculations predict a $6^-$ ground state and a group of states with spins and parities $3^-$, $4^-$, $5^-$, and $6^-$ above 300 keV. These states are part of the $\pi f_{5/2}$-$\nu g_{9/2}$ multiplet, with the $2^-$ and $7^-$ states lying higher in energy (above 500 keV). Note that the $J = j_\pi + j_\nu - 1 = 6^-$ state descends in the $N = 49$ isotonic chain as $Z$ decreases (see Fig. 31 in [16]) and becomes the lowest level of $^{80}$Ga. Collinear laser spectroscopy measurements in odd-$A$ Ga isotopes [20] reveal the changing nature of the ground-state spins for $^{79}$Ga ($J = 3/2$) and $^{81}$Ga ($J = 5/2$). From the measured magnetic moments the authors concluded that in both isotopes the dominating configuration is $\pi(f_{5/2})^3$. Therefore, for $^{80}$Ga one would expect that the dominant configuration arises from the coupling of one proton in this orbit to a neutron hole in the $g_{9/2}$ orbit.

A second negative-parity multiplet with spins $3^-$ to $6^-$ appears in $^{80}$Ga, with the $5^-$ state the lowest one, at around 200 keV. This multiplet arises from the coupling of $f^2_{5/2}p^1_{3/2}$ protons and $g^{-1}_{9/2}$ neutrons. Here the $J = j_\pi + j_\nu - 1 = 5$ state drops in energy along the $N = 49$ isotonic chain and becomes the lowest member of the multiplet when the configuration changes from a proton particle to a proton hole at $^{82}$As.

In addition, the jj44bpn interaction provides better estimations for both the energies and $\beta$ feeding of the proposed $(1^+)$ levels and $B(M2)$ of the 685.4-keV transition. The

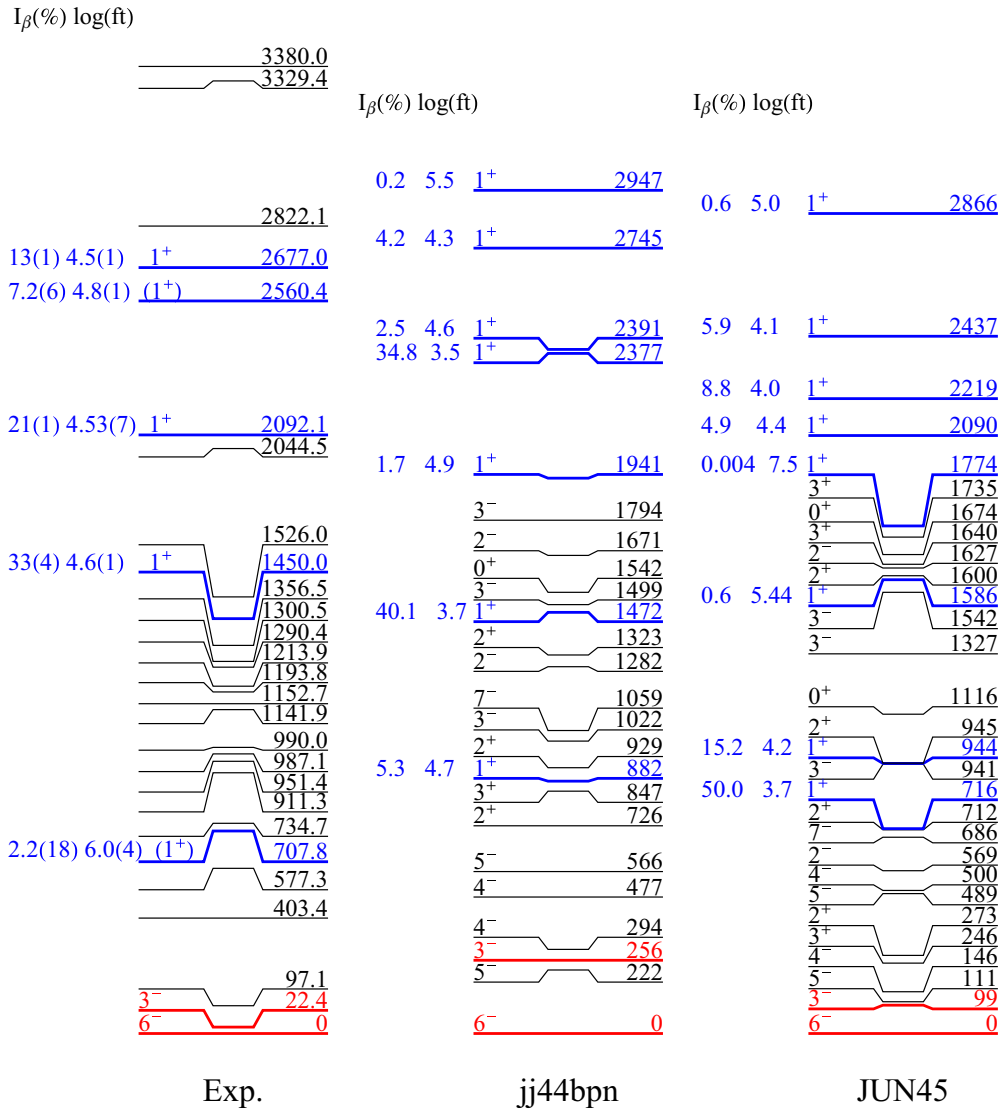


FIG. 4. (Color online) Comparison of the experimental levels (left) and shell-model calculations. The experimental level scheme is the same as the one presented in Fig. 1. The model space used for both interactions was $p_{3/2}f_{5/2}p_{1/2}g_{9/2}$. The region from 0 to 600 keV contains all the predicted levels. Due to high level density, the region from 600 to 1800 keV contains only the predicted levels with $J \leqslant 3$ and $J^\pi = 7^-_1$. The $>$ 1800-keV region contains only the levels with $J^\pi = 1^+$.

latter is predicted to be 0.11 W.u., which agrees well with the experimentally determined value of 0.6 W.u. The value calculated using the JUN45 interaction is a factor of 18 smaller. Quenched $g$ factors of $g_s = 0.7 g_{\text{free}}$ were used in these calculations; these were found in [3] to reproduce the magnetic moments of the ground states of neutron-rich Ga nuclei. The dominant configuration of the 707.8-keV, $(1^+)$ level is predicted to be $\pi f_{5/2}^3 \otimes \nu p_{1/2}^{-1}$ and that of the $3^-$ isomer $\pi f_{5/2}^3 \otimes \nu g_{9/2}^{-1}$, explaining the slow nature of transitions between these two states.

In Fig. 4, the $\beta$-feeding intensities of states in $^{80}$Ga, populated following the decay of the parent nucleus $^{80}$Zn, are shown. The predictions of the jj44bpn interaction are generally in better agreement with the experimental data than those of the JUN45 interaction. In particular, the strong $\beta$ feeding of the $1_2^+$ state is well reproduced by the calculations using the jj44bpn interaction. The $1_1^+$ state is, however, the strongest fed state when the JUN45 interaction is used, despite both interactions predicting similar dominant configurations for these two states.

## V. CONCLUSIONS

The present $\beta^-$ decay study brings significant new information regarding the structure of the neutron-rich $N = 49$ nucleus $^{80}$Ga. The spin and parity of the ground-state is firmly assigned to be $6^-$, and the previously unknown excitation energy of the low-lying isomer observed by collinear laser spectroscopy [3] is now fixed at 22.4 keV. This is in agreement with the ground-state assignment based on the shell-model calculations in [3,16]. A new isomeric level with a half-life of 18.3(5) ns was observed in the present experiment and is proposed as a candidate for the first $1^+$ state. A comparison between the measured and predicted half-life of this level and the $\beta^-$ feeding intensity distribution over the excited states of $^{80}$Ga proved to be a sensitive test of the shell-model interactions. The predictions of the jj44bpn interaction are in more reasonable agreement with the experimental data than the results obtained with JUN45.

## ACKNOWLEDGMENTS

This work was partially supported by the Spanish Ministry of Science and Innovation through Projects No. FPA2010-17142 and No. CSD-2007-00042 (CPAN Consolíder, Ingenio2010), by the Romanian ANCS/IFA Grant No. 6 ISOLDE, by the German BMBF under Grant No. 05P12PKFNE, and by the U.S. Department of Energy, Office of Nuclear Physics, under Grant No. DE-FG02-94ER40834. It was also partly funded by the NuPNET network FATIMA-NuPNET (PRI-PIMNUP-2011-1338) and by the European Union Seventh Framework through ENSAR (Contract No. 262010). We kindly acknowledge support from the ISOLDE Collaboration and the ISOLDE physics and technical groups. The fast-timing electronics was provided by the Fast Timing Pool of Electronics and MASTICON.

[1] R. Surman, M. Mumpower, R. Sinclair, K. L. Jones, W. R. Hix, and G. C. McLaughlin, AIP Adv. **4**, 041008 (2014).
[2] J. Hakala *et al.*, Phys. Rev. Lett. **101**, 052502 (2008).
[3] B. Cheal *et al.*, Phys. Rev. C **82**, 051302(R) (2010).
[4] D. Verney *et al.*, Phys. Rev. C **87**, 054307 (2013).
[5] U. Köster *et al.*, AIP Conf. Proc. **798**, 315 (2005).
[6] E. Bouquerel, R. Catherall, M. Eller, J. Lettry, S. Marzari, T. Stora, and ISOLDE Collaboration, Eur. Phys. J. Spec. Top. **150**, 277 (2007).
[7] U. Köster, O. Arndt, E. Bouquerel, V. N. Fedoseyev, H. Frånberg, A. Joinet, C. Jost, I. S. K. Kerkines, R. Kirchner, and Targisol Collaboration, Nucl. Instrum. Methods Phys. Res. B **266**, 4229 (2008).
[8] H. Mach, R. Gill, and M. Moszynski, Nucl. Instrum. Methods Phys. Res. A **280**, 49 (1989).
[9] M. Moszynski and H. Mach, Nucl. Instrum. Methods Phys. Res. A **277**, 407 (1989).
[10] J. A. Winger, J. C. Hill, F. K. Wohn, R. Moreh, R. L. Gill, R. F. Casten, D. D. Warner, A. Piotrowski, and H. Mach, Phys. Rev. C **36**, 758 (1987).
[11] B. Ekström, B. Fogelberg, P. Hoff, E. Lund, and A. Sangariyavanish, Phys. Scr. **34**, 614 (1986).
[12] A. Makishima, M. Asai, T. Ishii, I. Hossain, M. Ogawa, S. Ichikawa, and M. Ishii, Phys. Rev. C **59**, R2331 (1999).
[13] T. Kibédi, T. W. Burrows, M. B. Trzhaskovskaya, P. M. Davidson, and C. W. Nestor, Jr., Nucl. Instrum. Methods Phys. Res. A **589**, 202 (2008).
[14] P. Endt, At. Data Nucl. Data Tables **23**, 547 (1979).
[15] K. Sieja and F. Nowacki, Phys. Rev. C **81**, 061303 (2010).
[16] M. Honma, T. Otsuka, T. Mizusaki, and M. Hjorth-Jensen, Phys. Rev. C **80**, 064323 (2009).
[17] B. Brown and A. Lisetskiy (unpublished).
[18] P. C. Srivastava, J. Phys. G: Nucl. Part. Phys. **39**, 015102 (2012).
[19] B. A. Brown, W. D. M. Rae, E. McDonald, and M. Horoi, NUSHELLX@MSU, http://www.nscl.msu.edu/~brown/resources/resources.html (http://www.garsington.eclipse.co.uk, ed.), NuShellX, W. D. M. Rae.
[20] B. Cheal *et al.*, Phys. Rev. Lett. **104**, 252502 (2010).
[21] G. Audi, A. Wapstra, and C. Thibault, Nucl. Phys. A **729**, 337 (2003).